Draft version September 7, 2026
Typeset using LaTeX **RNAAS** style in AASTeX631

A Multi-Epoch Reflected-Light Search for Wildfires and Forest Recovery on Terrestrial Exoplanets

Szilárd Csizmadia[1]

[1] *Institute of Planetary Research, German Aerospace Center (DLR), Rutherfordstrasse 2, 12489 Berlin, Germany*

ABSTRACT

I propose a differential, multi-epoch search for catastrophic wildfire and subsequent ecosystem recovery on forest-dominated terrestrial exoplanets. The strongest observable is not a small change in atmospheric CO_2 measured in transmission, but a temporally ordered combination in directly imaged reflected light: rapid smoke and CO enhancement, a persistent wavelength-dependent albedo change at a fixed rotational phase, weakening of a pre-existing photosynthetic reflectance edge, and gradual restoration of the surface spectrum. Terrestrial Landsat measurements show that severe fires can change local NIR and SWIR reflectance by about 0.1. In a linear areal-mixing approximation, a one-percent projected burned fraction therefore produces disk-integrated single-band albedo perturbations of order 10^{-3}. A future kilometer-class filled-aperture observatory could perform the full time-domain experiment.

CONCEPT AND NOVELTY

Vegetation-like spectral edges, wavelength-dependent surface retrieval, rotational mapping, atmospheric seasonality, biomass-related atmospheric chemistry, and transient aerosols have all been studied separately (Seager et al. 2005; Kawahara & Fujii 2011; Gomez Barrientos et al. 2023; Burr et al. 2026; Olson et al. 2018; Misra et al. 2015). Biomass emissions can modify O_2, O_3, CH_4, N_2O, and CH_3Cl in modeled Earth-like atmospheres (Grenfell et al. 2014; Gebauer et al. 2021), while biomass burning contributes CO (Schwieterman et al. 2019). I propose combining these established ingredients into a falsifiable time-domain sequence: an impulsive atmospheric transient, a long-lived surface scar recurring at the same rotational phase, and recovery on an ecological timescale. The novel observable is therefore the *disturbance–localization–recovery* pattern rather than any individual molecule or color.

For observations matched in orbital phase α and rotational phase ϕ, define

$$\mathcal{D}(\lambda, \phi, t) = \frac{F_{\rm p}(\lambda, \phi, t) - F_{\rm p,0}(\lambda, \phi)}{F_{\rm p,0}(\lambda, \phi)}, \tag{1}$$

Here $F_{p,0}$ is a multi-orbit reference,λ is wavelength, F_p is the planetary flux, and t is time. A minimal surface perturbation is

$$\Delta A_{\rm eff,\lambda}(t) \simeq f_{\rm b}(t)\,[\rho_{\lambda,\rm burn} - \rho_{\lambda,\rm forest}] + \Delta A_{\lambda,\rm smoke}(t). \tag{2}$$

where $A_{\rm eff,\lambda}$ is the disk-integrated apparent albedo, ρ_λ is the local surface reflectance, and f_b is the effective projected fraction of the illuminated visible disk covered by burned forest. An NIR–SWIR diagnostic analogous to a terrestrial burn index is

$$I_{\rm burn}(t) = \frac{A_{\rm NIR}(t) - A_{\rm SWIR}(t)}{A_{\rm NIR}(t) + A_{\rm SWIR}(t)}. \tag{3}$$

Here we use NIR for the near-infrared range 0.7–1.4 μm and SWIR for the short-wave infrared range 1.4–3 μm. The optimal bands should be inferred from the planet's persistent pre-event reflectance spectrum rather than fixed a priori to terrestrial chlorophyll features or any other model assumptions.

WHY REFLECTED-LIGHT MONITORING IS FAVORED

For this particular science case, multi-epoch wavelength-dependent albedo measurements are intrinsically more informative than transit spectroscopy. Transmission spectroscopy samples only the atmospheric annulus at the terminator and has little direct sensitivity to a localized burn scar or to the loss and recovery of a surface reflectance edge. A

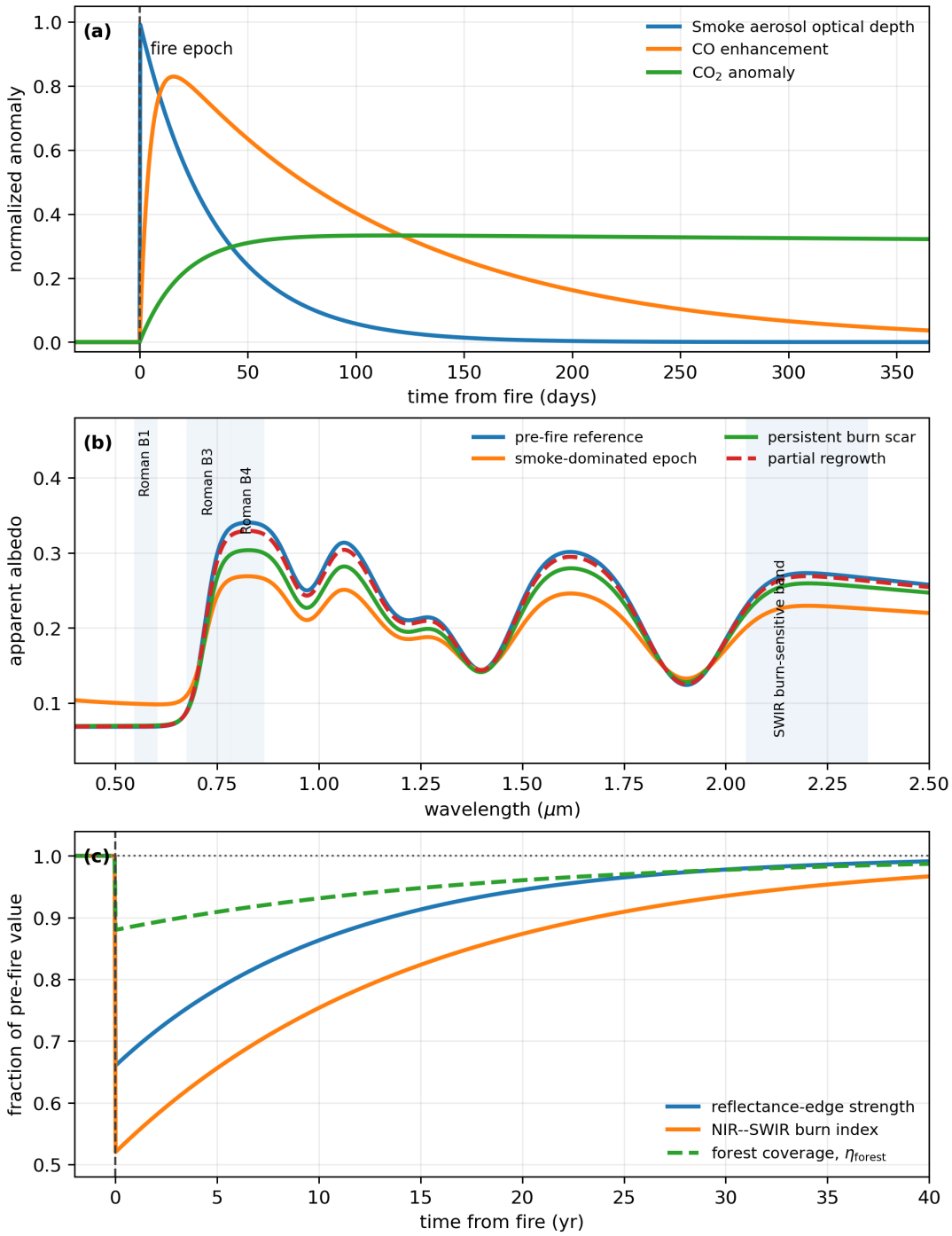


Figure 1. Schematic, dimensionless wildfire sequence; the curves are not radiative-transfer predictions. (a) Smoke and CO respond rapidly, whereas a carbon anomaly may persist. (b) Multi-epoch apparent-albedo spectra distinguish a smoke-dominated epoch, a persistent burn scar, and partial regrowth. The current Roman Coronagraph Band 1, Band 3, and Band 4 passbands are indicated near the terrestrial-like reflectance edge; a separate SWIR band would be needed for a stronger burn diagnostic. (c) A reflectance-edge index and an NIR–SWIR burn index fall abruptly and recover more slowly than the atmospheric tracers. A genuine surface anomaly should recur at the same rotational phase.

regional fire is also diluted through the atmosphere, while the effective transmission altitude of an absorber varies approximately as $\Delta z \simeq H \ln(x_2/x_1)$, where H is the atmospheric scale height and x_1 and x_2 are the absorber volume

mixing ratios at the two epochs. Detecting a modest CO_2 or CO change therefore requires differencing already weak atmospheric features between transits, often at a cadence of only one transit per orbit for temperate planets.

Direct imaging instead measures the illuminated disk and can be scheduled at many orbital and rotational phases. Terrestrial Landsat data provide an empirical scale for the surface term. For burned areas, Koutsias et al. (2013) measured TM4 NIR reflectance falling from 0.22327 to 0.13495 and TM7 SWIR reflectance rising from 0.11820 to 0.23441. Thus $|\Delta\rho_{\rm NIR}| = 0.0883$, $\Delta\rho_{\rm SWIR} = 0.1162$, and the NIR–SWIR color $\rho_{\rm NIR} - \rho_{\rm SWIR}$ changed by 0.2045. These values are not universal, but demonstrate order of ~ 0.1 local spectral perturbations after severe fire. For $f_{\rm b} = 0.01$, linear areal mixing gives $|\Delta A_{\rm eff,NIR}| \simeq 8.8 \times 10^{-4}$ and $\Delta A_{\rm eff,SWIR} \simeq 1.16 \times 10^{-3}$. If the relevant apparent planetary albedo is of order 0.2, these correspond to relative isolated-planet flux changes of about 0.4–0.6%. Multi-band monitoring can simultaneously test weakening of a reflectance edge, a burn-sensitive color change, and persistence at fixed ϕ. Transmission spectra remain valuable as a complementary search for CO, smoke aerosols, and other combustion products, but reflected-light spectrophotometry should be the primary observable.

ATMOSPHERIC CONTEXT AND FALSE POSITIVES

Combustion itself has also been considered in exoplanet atmospheres. Grenfell et al. (2018) showed that suitable H_2–O_2, CO–O_2, or CH_4–O_2 mixtures can approach combustion–explosion limits. This provides both a compositional boundary condition and an unusual false-positive scenario. Atmosphere-wide combustion should cause a predominantly global chemical transition; a surface wildfire should additionally create a phase-localized albedo anomaly followed by regrowth. Host-star UV irradiation must also be constrained because it controls the photochemical response and decay times of CO, CH_4, and related species (Grenfell et al. 2014).

Clouds should decorrelate across rotations. Dust storms and volcanic aerosols may persist, but need not produce a co-located loss and later restoration of a pre-existing photosynthetic surface component. The temporal ordering therefore supplies much of the discriminating power.

ROMAN PATHFINDER AND KILOMETER-CLASS PROGRAM

The Nancy Grace Roman Space Telescope cannot perform this experiment on an Earth–Sun analog: the Roman Coronagraph has a formal Band 1 requirement of 10^{-7} contrast at 575 nm, with expected performance extending toward 10^{-8}, whereas an Earth twin in reflected visible light is near 10^{-10} (Bailey et al. 2023; Roman Science Support Center 2026). Roman is nevertheless a particularly relevant pathfinder. Here, "pathfinder" means demonstrating the required high-contrast differential-photometry methodology, not detecting exoplanet wildfires. Its current modes include 575 nm imaging, best-effort $R \sim 50$ spectroscopy centered near 730 nm (approximately 680–780 nm), and best-effort 825 nm imaging/polarimetry (Roman Science Support Center 2026); these bands sample both sides of a terrestrial-like red edge.

Roman can test repeatable differential photometry of a coronagraphically isolated planet, chromatic speckle calibration, wavefront stability, reference-star subtraction, and the separation of intrinsic albedo variability from orbital phase. Joint reflected-light photometry and astrometry can improve orbital constraints (Molina et al. 2026), enabling $\Phi[\alpha(t)]$ to be modeled before searching for intrinsic variability. Roman polarimetry and circumstellar-dust measurements can further quantify two important degeneracies for future exo-Earth monitoring: aerosol/cloud scattering and structured exozodiacal background.

For the full experiment, a baseline should contain 6–12 orbital epochs, each covering a rotation with roughly 8–12 phase bins. Spectroscopy over 0.4–2.5 μm at $R \sim 50$–100 would measure the reflectance edge, atmospheric H_2O and CO near 2.35 μm, and an NIR–SWIR burn diagnostic; 3–5 μm coverage would add active-fire thermal emission and CO near 4.6 μm. After a candidate event, weekly-to-monthly observations would follow smoke and CO, with yearly observations testing regrowth.

A filled 1 km aperture has enormous photon leverage and the KST concept was explicitly developed as a photon-rich optical/IR/millimeter observatory (Johnson & Crowe 2021; NASA 2018). For a representative $\sim 0.5\%$ single-band planetary-flux perturbation, a 5σ differential detection requires approximately 0.1% repeatability, or S/N ~ 1000 in a suitably combined spectral/phase bin. The main challenge is therefore likely not photon statistics but repeatable starlight suppression near 10^{-10}, chromatic wavefront stability, stellar-variability removal, exozodiacal subtraction, and 10^{-3}-level calibration of the isolated planetary spectrum.

The immediate quantitative next step is an Earth-as-an-exoplanet injection–recovery experiment using real satellite maps and spectra before, during, and after major wildfires. Disk integration, realistic clouds, phase sampling, and

instrument noise can then determine the minimum detectable $f_{\rm b}$ as a function of forest coverage, distance, cadence, and aperture. This would convert the proposed observing concept into testable requirements for future kilometer-class exoplanet observatories.

REFERENCES

Bailey, V. P., et al. 2023, Proc. SPIE, 12680, 126800T

Burr, Z., Damiano, M., Kofman, V., Hu, R., & Villanueva, G. L. 2026, ApJ, 1001, 222

Gebauer, S., Vilović, I., Grenfell, J. L., Wunderlich, F., Schreier, F., & Rauer, H. 2021, ApJ, 909, 128

Gomez Barrientos, J., MacDonald, R. J., Lewis, N. K., & Kaltenegger, L. 2023, ApJ, 946, 96

Grenfell, J. L., Gebauer, S., von Paris, P., Godolt, M., & Rauer, H. 2014, Planet. Space Sci., 98, 66

Grenfell, J. L., Gebauer, S., Godolt, M., Stracke, B., Lehmann, R., & Rauer, H. 2018, ApJ, 861, 38

Johnson, T. P., & Crowe, D. G. 2021, Appl. Opt., 60, 3464

Kawahara, H., & Fujii, Y. 2011, ApJL, 739, L62

Koutsias, N., Pleniou, M., Mallinis, G., Nioti, F., & Sifakis, N. I. 2013, Int. J. Remote Sens., 34, 7049

Misra, A., Krissansen-Totton, J., Koehler, M. C., & Sholes, S. 2015, Astrobiology, 15, 462

Molina, F., Blunt, S., & Wang, J. 2026, arXiv:2607.22754

NASA 2018, Kilometer Space Telescope (KST), NASA Innovative Advanced Concepts Phase II

Olson, S. L., Schwieterman, E. W., Reinhard, C. T. et al. 2018, ApJL, 858, L14

Roman Science Support Center 2026, Roman Coronagraph Primer

Schwieterman, E. W., et al. 2019, ApJ, 874, 9

Seager, S., Turner, E. L., Schafer, J., & Ford, E. B. 2005, Astrobiology, 5, 372